New evaluation of ship mooring with friction effects on mooring rope and cost-benefit estimation to improve port safety

Lee, Sang-Won

Sasa, Kenji

Aoki, Shin-ich

Yamamoto, Kazusei

Chen, Chen

(Citation)
International Journal of Naval Architecture and Ocean Engineering,13:306-320

(Issue Date)
2021

(Resource Type)
journal article

(Version)
Version of Record

International Journal of Naval Architecture and Ocean Engineering 13 (2021) 306–320

Contents lists available at ScienceDirect

International Journal of Naval Architecture and Ocean Engineering

journal homepage: http://www.journals.elsevier.com/international-journal-of-naval-architecture-and-ocean-engineering/

New evaluation of ship mooring with friction effects on mooring rope and cost-benefit estimation to improve port safety

Sang-Won Lee [a], Kenji Sasa [a,*], Shin-ich Aoki [b], Kazusei Yamamoto [c], Chen Chen [d]

[a] Graduate School of Maritime Sciences, Kobe University, Kobe, Hyogo, Japan
[b] Graduate School of Engineering, Osaka University, Suita, Osaka, Japan
[c] Marine Technical College, Japan Agency of Maritime Education and Training for Seafarers, Ashiya, Hyogo, Japan
[d] School of Navigation, Wuhan University of Technology, Wuhan, China

ARTICLE INFO

Article history:
Received 28 November 2020
Received in revised form
21 March 2021
Accepted 6 April 2021
Available online 10 May 2021

Keywords:
Mooring problem
Long-period waves
Wave forecast
Rope damage
Optimal mooring

ABSTRACT

To ensure safe port operations around the world, it is important to solve mooring problems. In particular, the many ports that face open seas have difficulties with long-period waves. As a countermeasure, the installation of a breakwater is proposed for mooring safety. However, this often cannot be put into practice because of financial issues. Instead, port terminals control berthing schedules with weather forecasting. However, mooring problems remain unsolved, because of inaccurate wave forecasting. To quantify the current situation, numerical simulations are presented with ship motions, fender deflections, and rope tensions. In addition, novel simulations for mooring ropes are proposed considering tension, friction, bending fatigue, and temperature. With this novel simulation, the optimal mooring method in terms of safety and economic efficiency was confirmed. In terms of safety, the optimal mooring method is verified to minimize dangerous mooring situations. Moreover, the optimal mooring method shows economic benefits and efficiency. It can help to reinforce the safety of port terminals and improve the efficiency of port operations.

1. Introduction

Around the 1990s, with cargo volume increasing around the world, port efficiency and the safety of ships in ports became important. As such, many studies have investigated the behavior of moored ships through physical experiments, numerical simulations, and field observations (Kubo and Barthel, 1992; PIANC, 1995; Shiraishi et al., 1999). Kubo and Sakakibara (1999) proposed the expansion of breakwaters and improvement of the mooring system as countermeasures to mooring issues. With countermeasures, such as the expansion of breakwaters, it was expected that mooring problems could be solved. However, the economic slowdown in the 2000s, such as in the global economic crisis, hindered the progress of measures that incur large-scale construction costs.

In addition, the influence of waves, such as long-period waves and harbor resonance has been identified as the main cause of large ship motions. By controlling of the natural period and spring constant between mooring lines and fenders, it can reduce ship motions. It is more advantageous to use High-Modulus Poly Ethylene (HMPE) ropes, which have a low stretch of about 3–5%, rather than conventional synthetic fiber ropes, such as nylon and Poly-Propylene (PP) ropes with a high elasticity of about 20–30% (Foster, 2002; Villa-Caro et al., 2018). However, these HMPE ropes are not adopted by many shipping companies yet owing to various disadvantages, such as high price and vulnerability to high temperatures.

Even after 20 years, many ports suffer from mooring difficulties due to these reasons (Van der Molen et al., 2006, 2015; Kwak et al., 2012; López and Iglesias, 2014; Sasa et al., 2018, 2019). Sasa (2017) found that coastal passenger ships mooring at islands, which are exposed to the ocean, have been placed in dangerous conditions by long-period waves.

Harbors exposed to dangerous situations have used the weather forecast system as an alternative to reduce mooring risks by evacuating ships from piers when rough weather is predicted (Shiraishi, 2009; Yoneyama et al., 2017). However, weather forecasts cannot always be accurate, and these failures of forecasts have resulted not only in additional offshore anchoring, leading to additional losses,

* Corresponding author.
E-mail address: sasa@maritime.kobe-u.ac.jp (K. Sasa).
Peer review under responsibility of The Society of Naval Architects of Korea.

https://doi.org/10.1016/j.ijnaoe.2021.04.002

but also mooring accidents caused by unpredicted rough waves.

Previous studies on mooring problems have only focused on the tension of the mooring rope (Van der Molen et al., 2006; Sakakibara and Kubo, 2009; Sasa et al., 2018, 2019). However, several studies have confirmed heat generation when cyclic tension is applied to the rope (Karnoski and Liu, 1988; Hearle et al., 1993; Overington and Leech, 1997; Black et al., 2012), especially in the HMPE rope. Even if the applied tension does not exceed the safety threshold of the mooring rope, the repeatedly applied forces eventually damage the ropes with heat generation because of the accumulation of friction energy (Yamamoto et al., 2004, 2006; Yamamoto, 2007). In addition, the bending fatigue largely affects ropes. (Hobbs and Burgoyne, 1991; Nabijou and Hobbs, 1995; Sloan et al., 2003; Bossolini et al., 2016; Ning et al., 2019).

In this study, we developed a new evaluation of cost-benefit performance to plan an optimal mooring method that satisfies the safety and economic efficiency for port operations. For more accurate safety evaluation of mooring ropes, an improved temperature evaluation method considering frictions and bending fatigues was used instead of the tension evaluation method. Subsequently, new parameters such as demurrage, initial investment cost, and maintenance cost were introduced to verify the economic efficiency. The results show that the proposed methods can reflect the actual situations and the effects of changing the mooring arrangement and rope material. Hence, this paper presents numerical methods for evaluating mooring safety as well as practical applications. Specifically, this study can improve port efficiency from the viewpoint of both safety and economic efficiency.

Following this introductory information, Section 2 presents a nationwide questionnaire and current berthing operations to understand and identify actual mooring problems. In Section 3, we describe the methods used to calculate the moored ship motions and the detailed process to assess mooring safety developed. In Section 4, we introduce simulation conditions such as the target vessel, mooring arrangements and the weather conditions in the study area. The results and application for moored ship safety in rough sea conditions are discussed in Section 5, and concluding remarks, key findings from this study, and suggested directions for future research are presented in Section 6. Fig. 1 illustrates the flowchart of how mooring methods is evaluated on the viewpoint of safety and economic efficiency in this study. Various parameters should be included in the design of mooring methods.

2. Investigation of current mooring problems

2.1. Nationwide questionnaire and survey on mooring problem

In the 1990s, mooring accidents were reported in ports worldwide. Many studies have shown that these accidents are mainly caused by long-period waves (Sasa et al., 2001; Hashimoto and Kawaguchi, 2003; Van der Molen et al., 2006, 2015; González-Marco et al., 2008; Shiraishi, 2009; Ikeda et al., 2011; Van Essen et al., 2013; López and Iglesias, 2014). Thus, the following methods are proposed as countermeasures: (1) Construction of additional breakwaters, (2) Control of the spring constants between mooring lines and fenders to reduce asymmetrical property of mooring, (3) Control the natural period of motions to avoid resonance phenomena.

These practical methods are expected to be used for the safety of port operations. However, they cannot be put into practice because of the large budget required for construction costs. It is necessary to study this current situation on mooring problems from the viewpoint of port operation. A nationwide survey was conducted to accurately identify the current mooring problems. The survey was conducted by mailing a questionnaire sheet. The questionnaire was administered to 120 organizations related to port operations, such as ship operating companies, port agencies, and local governments. The number of responders is 42 (35%). The total number of questions is 8, including the main questions (Q1)–(Q4), which were as follows:

- (Q1) Have you ever experienced difficulties or dangers in port operation caused by rough seas?
- (Q2) Are you aware of research related to mooring problems conducted over the decades?
- (Q3) Do you use the weather forecast service for port safety management?
- (Q4) Do you think current management is sufficient for the safe operation of moored ships?

Fig. 2 shows the answers to questions (Q1)–(Q4). In (Q1), 63% of the respondents said they experienced mooring difficulties due to

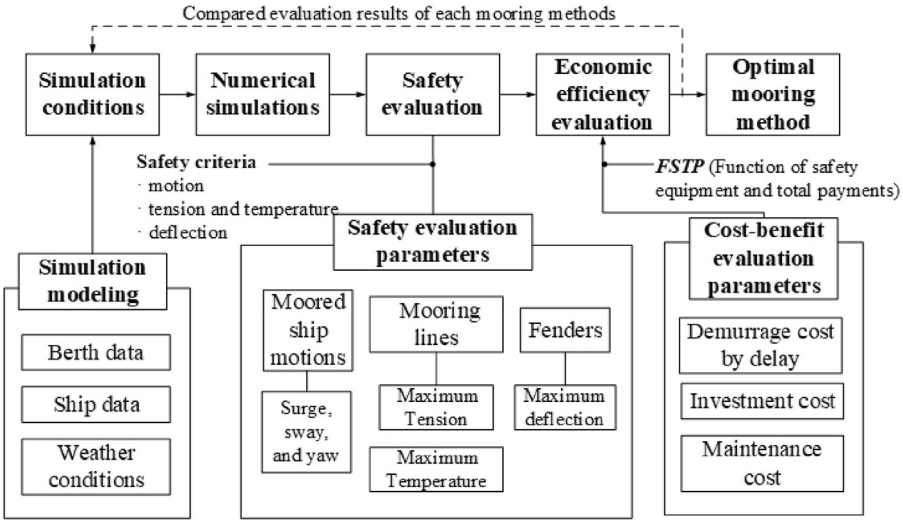

Fig. 1. Flowchart of the optimal mooring method process.

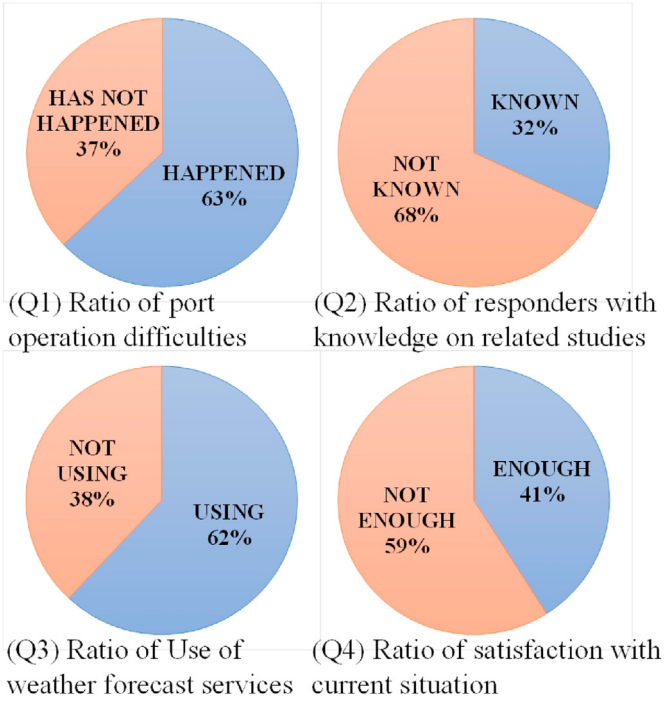

Fig. 2. Questionnaire results.

large ship motions caused by waves. In (Q2), nearly 70% of the respondents were not aware of related studies on moored ship motions. Moreover, it was found that most of the respondents misunderstood the definition of long-period waves (30–300 s of wave periods) with swells (10–16 s). As an alternative to the countermeasure, 62% of the respondents use weather forecast services, as shown in (Q3). This means that nearly 40% of respondents still operate ships without weather forecasts for mooring safety. Regarding (Q4), 59% of the respondents feel insufficiently equipped for the current situation of moored ship motions.

As a result of the nationwide survey, the relevant operators are still struggling with the problems of moored ships. Accordingly, it is necessary to prepare more realistic countermeasures. It is evident that related studies have not been applied to improve the safety of mooring ship operations in ports. In addition, it indicates that mooring problems are not being resolved from a political and economic perspective. Therefore, it is necessary to conduct further research from this point of view.

2.2. Current berthing operation in T port

A specific port should be selected to analyze moored ship motions with long-period waves. The selected port is T Port, which is one of the main ports facing the Pacific Ocean with breakwaters to prevent wave effects (Fig. 3). The visiting survey in T Port was conducted three times—in October 2017, March 2018, and March 2019—to investigate the real mooring problems. The breakwaters were to be expanded as per a decision of the local committee to maintain port safety. However, the construction has not been affected due to financial deficits. One of the operators of this port, which has problems with the influence of long-period waves, has been using weather forecasting services as an alternative to breakwater expansion since 2011.

Waves and winds are continuously observed with an ultrasonic wave gauge and wind sensor at the end of the port. The height of the sea surface is recorded at 0.5 s intervals. Additionally, the time series in terms of the power spectrum is statistically analyzed. The heights of the significant and long-period waves can be obtained as follows:

$$H_{1/3} = 4.0\sqrt{\int_0^{\infty} S(f)df}, H_{L1/3} = 4.0\sqrt{\int_0^{0.03} S(f)df} \quad (1)$$

where $H_{1/3}$ and $H_{L1/3}$ are the wave heights of the significant and long-period waves, respectively, $S(f)$ is the frequency spectrum of waves inside the harbor, and f is the frequency. Fig. 4 shows the (A) time history and (B) power spectrum of measured wave data inside the harbor. From the power spectrum graph in Fig. 4(B), it can be seen that a low frequency of 0.006–0.02 Hz (50–166 s) has strong power spectrums inside the harbor. This shows the presence of the

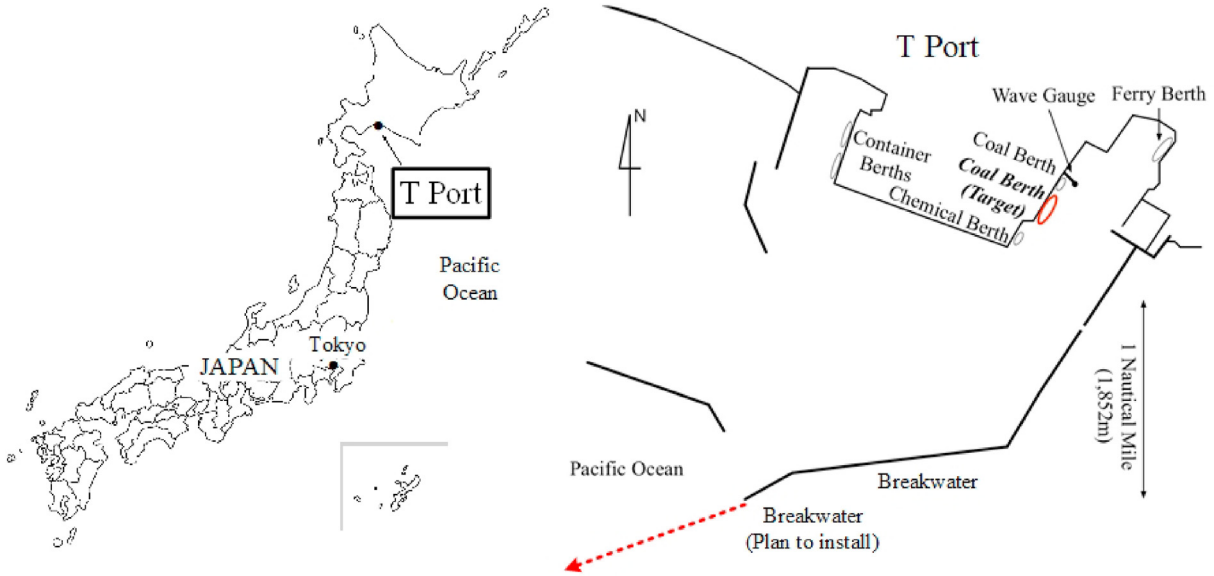

Fig. 3. Study area facing the open sea (Pacific Ocean) and the detailed port terminal status for breakwater installation and expansion plans.

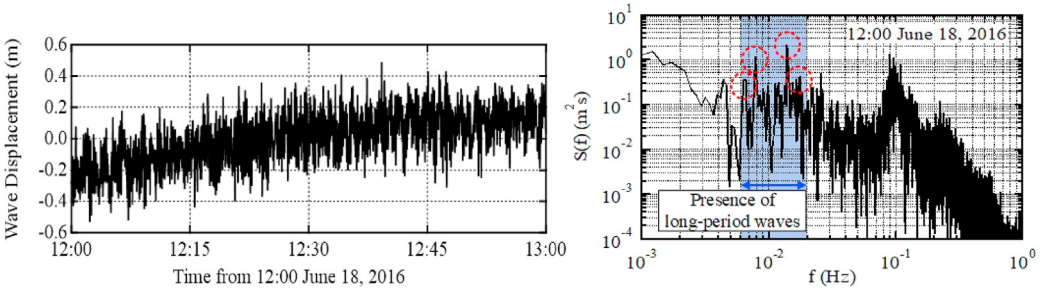

(A) Time history for wave inside harbor at 12:00 June 18, 2016 (B) Power spectrum for wave inside harbor at 12:00 June 18, 2016

Fig. 4. Time history and wave spectrum in terms of the power spectrum inside T Port.

Table 1
Berthing operation guidelines and standards for moored ships in T Port.

Wave level	Action in the port	Decision by berth master
Level 1	Pay attention during cargo handling (Caution and additional mooring lines)	Staying inside harbor with caution
Level 2	Cargo handling impossible (Danger)	Offshore anchoring
Level 3	Dangerous and emergency evacuation is required (Urgency)	

long-period waves near the mooring facilities.

In this terminal, the berth masters, who have managed and operated the berthing of ships, determine the berthing schedule, and refer to the wave forecasting service. The Ministry of Land, Infrastructure, Transport and Tourism (MLIT) (2009) recommends the operation standards as a significant wave height in the 0.3–0.5 m range and long-period waves in the 0.1–0.2 m range. Based on these recommendations for weather forecasting, each wave condition is divided into three levels, as shown in Table 1.

In "Level 1," the ships can stay inside the harbor with caution. In "Level 2" and "Level 3," all ships in the port must immediately evacuate to offshore anchorage. With these berthing operation guidelines, serious accidents have been avoided. However, dangerous situations still occur because of incorrect forecasts.

3. Numerical simulation of moored ship motions

3.1. Analytical theory of moored ship motions

The numerical analysis for the motion of a ship moored to a quay wall induced by environmental forces was conducted by solving the equations of motion in Eq. (2) (Cummins, 1962). The time domain analysis was applied for this numerical analysis. In previous studies, this model was validated for multiple cases of measured ship motions with long-period waves at various ports with accuracy (Kubo and Sakakibara, 1999; Shiraishi et al., 1999). In this study, since the moored ship motion could not be measured in the T Port, the evaluation was conducted as the simulated ship motion. The ship motion was simulated based on the measured wave data inside the harbor. Moreover, it can be assumed that the estimated ship motion was reliable by comparing it with the visual report in T Port.

$$\sum_{i=1}^{6}(M_{ij}+m_{ij}(\infty))\ddot{X}_j(t)+\sum_{i=1}^{6}\times\int_{-\infty}^{t}L_{ij}(t-\tau)\dot{X}_j(\tau)d\tau+\sum_{i=1}^{6}(C_{ij}+K_{ij})X_j(t)=F(t)(i,j=1,2,\cdots,6), \tag{2}$$

where M is the mass matrix (including the moment of inertia) of the hull; $m(\infty)$ is the invariant additional mass; $L(t)$ is the memory effect function; C is the stability matrix; K is the mooring force matrix; $F(t)$ is the external force vector at time t; X indicates the displacement vector of ship motion; and the subscripts i and j indicate the motion mode. Furthermore, $L(t)$ and $m(\infty)$ are expressed by the following equations:

$$L_{ij}(t)=\frac{2}{\pi}\int_0^{\infty}q_{ij}(\omega)cos\omega t d\omega, \tag{3}$$

$$m_{ij}(\infty)=p_{ij}(\omega)+\frac{1}{\omega}\int_0^{\infty}L_{ij}(t)sin\omega t dt, \tag{4}$$

where $p(\omega)$ and $q(\omega)$ are the added mass and the damping coefficient at the angular frequency ω. The wave existing force is a combination of wave components in each frequency and wave direction on the actual sea surface. They are computed using the three-dimensional Green function method (John, 1950) for arbitrary body shape in each angular frequency. This numerical model reproduces the accurate moored ship motions for some measured cases in long-period waves (Shiraishi et al., 1999). Eq. (2) is defined in the time domain and is numerically solved by the Newmark-β method.

Each case was solved for 3600 s with a time interval of 0.2 s. The amplitude of ship motions is defined as the maximum amplitude using the zero-up crossing method. The tension of the mooring rope and fender deformation is evaluated as the maximum value in the computed time series.

The tension of the mooring rope is also an important parameter for evaluating the safety of a moored ship. The absolute value of the rope tension has been used as a parameter to discuss safety (Shiraishi et al., 1999). In OCIMF (2018), the safety working load (SWL) of synthetic fiber rope is defined as 50% of the Minimum Breaking Load (MBL). The ratio of the applied tension to the MBL of the rope can be defined as the probability of breakage by tension *PBT*, defined as

$$PBT(\%) = \frac{T_m}{T_{MBL}}, \tag{5}$$

where T_m is the maximum value of the affecting tension of the mooring rope, and T_{MBL} is the specific MBL of the rope, which denotes the allowable load. Referring to previous studies related to the rope-breaking mechanism (Karnoski and Liu, 1988; Hearle et al., 1993; Overington and Leech, 1997), friction is also an important factor in rope safety. The probability of breakage without consideration of friction can be underestimated. Therefore, it is necessary to develop the mooring evaluation method considering the friction.

3.2. Analysis of mooring rope temperature

The tension of the mooring rope occurs periodically under the influence of waves. This repetitive tension can eventually lead to a temperature rise or breakage of the rope. The thermal calculation needs to divide the two parts of the rope: (1) straight part and (2) bending part, as shown in Fig. 5. In the straight part, friction occurs between strands inside the rope, so mainly internal friction is generated. In the bending part, however, in addition to the internal friction, external friction is generated because of contact between the structure, such as the fairlead and the surface of the rope. In addition, this bending part is subject to the effect of bending fatigue.

First, it is possible to calculate the frictional energy of the straight parts based on previous experiments (Yamamoto et al., 2004, 2006; Yamamoto, 2007). For heat calculation by internal friction, it is necessary to use the thermal equilibrium equation as follows:

$$dQ_{i+1,j} = dQ_{i,j-1} - dQ_{i,j} + dQ_{fri,j}, \tag{6}$$

where $dQ_{i+1,j}$ is the accumulated heat quantity, $dQ_{i,j-1}$ is the inflow heat quantity, $dQ_{i,j}$ is the outflow heat quantity, and $dQ_{fri,j}$ is the heat quantity due to friction. i and j are the time and position from the inside of the rope, respectively. The accumulated heat quantity, inflow, and outflow heat quantity can be calculated by the equation for heat conductivity as follows:

$$dQ_{i+1,j} = c\rho V_j(\theta_{i+1,j} - \theta_{i,j}), \tag{7}$$

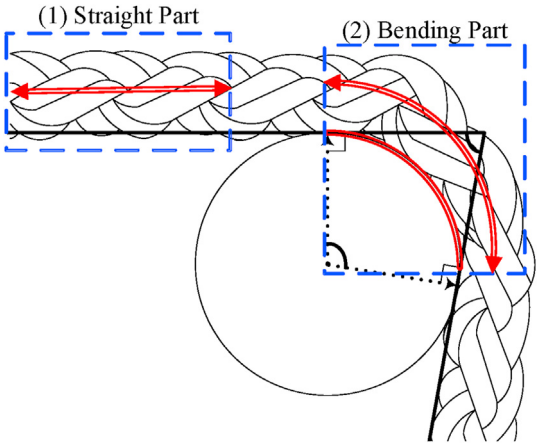

Fig. 5. Classification of parts subject to friction: (1) straight part and (2) bending part.

$$dQ_{i,j-1} = \lambda A_{j-1}\frac{\theta_{i,j-1} - \theta_{i,j}}{dr}dt, \tag{8}$$

$$dQ_{i,j} = \lambda A_j\frac{\theta_{i,j} - \theta_{i,j+1}}{dr}dt, \tag{9}$$

where c is the specific heat of the rope ($kcal/^\circ C \cdot kg$), ρ is the density (kg/m^3), V_j is the volume of position j, and A_j is the area of the section. λ is the heat conductivity coefficient and $\theta_{i,j}$ is the temperature in time i and position j, r is the radius of the rope, dr is $r/10$, and dt is 0.5 s, which is the time interval used in this study. In addition, the internal frictional energy can be calculated by the following:

$$dQ_{fri,j} = \frac{k_1 \cdot k_2 \cdot k_3 \cdot \mu \cdot A_s \cdot p_i \cdot dl_i}{4.186 \times 10^3} \cdot \frac{V_j}{V}, \tag{10}$$

where k_1 is the coefficient of pressure, k_2 is the coefficient of elongation, and k_3 is the coefficient of internal friction. These coefficients were obtained from the experiments. μ is the coefficient of friction, A_s is the total area of the contact area (m^2), p_i is the internal pressure (N/m^2), dl_i is the line elongation, V_j is the volume of j position, and V is the total volume of the rope. The temperature of the rope by internal friction can be obtained by the following:

$$\begin{aligned} c\rho V_j(\theta_{i+1,j} - \theta_{i,j}) = {} & \lambda A_{j-1}\frac{\theta_{i,j-1} - \theta_{i,j}}{dr}dt - \lambda A_j\frac{\theta_{i,j} - \theta_{i,j+1}}{dr}dt \\ & + \frac{k_1 \cdot k_2 \cdot k_3 \cdot \mu \cdot A_s \cdot p_i \cdot dl_i}{4.186 \times 10^3} \cdot \frac{V_j}{V}, \end{aligned} \tag{11}$$

where $\theta_{i,j}$ is the calculated temperature in i time and j position. This equation for the internal friction has been verified by experiments (Yamamoto et al., 2004, 2006; Yamamoto, 2007). However, this equation only explains for the straight part of the rope. Therefore, it is necessary to consider the additional frictional energy in the bending part of the rope. The additional frictional energy is generated by the external friction between the fairlead and the surface of the rope. It can be obtained by the Capstan equation, as shown in Eq. (12).

$$W_{ex} = T_m \cdot exp^{\mu\delta} \cdot dl, \tag{12}$$

where W_{ex} is the frictional energy of the external force between the fairlead and the rope, T_m is the tension of the rope, μ is the coefficient of friction, δ is the angle of the contact area, and dl is the elongation of the rope.

Finally, there is an effect of bending fatigue. Many studies have found that bending fatigue has a remarkable influence on the damage and heat of the rope (Nabijou and Hobbs, 1995; Sloan et al., 2003; Bossolini et al., 2016; Ning et al., 2019). Ridge et al. (2015) experimentally provided comparative results of the temperature rise through repeated load experiments on the bending part of synthetic fiber ropes. Through their experiments, the appropriate bending coefficient is added as k_4 to the equation of frictional energy in Eq. (13). The final result of the thermal model is summarized in Eq. (13), including both the internal friction, external friction, and bending fatigue.

$$\begin{aligned} c\rho V_j(\theta_{i+1,j} - \theta_{i,j}) = {} & \lambda A_{j-1}\frac{\theta_{i,j-1} - \theta_{i,j}}{dr}dt - \lambda A_j\frac{\theta_{i,j} - \theta_{i,j+1}}{dr}dt \\ & + \frac{k_1 \cdot k_2 \cdot k_3 \cdot k_4 \cdot \mu \cdot A_s \cdot p_i \cdot dl_i}{4.186 \times 10^3} \cdot \frac{V_j}{V} + T_m \cdot exp^{\mu\delta} \cdot dl, \end{aligned} \tag{13}$$

The maximum temperature rises in the bending parts owing to the additional external friction and bending fatigue, while the temperature rise in the straight parts only depends on the internal friction. The temperature of the bending part was compared to the maximum temperature for the safety parameter in this study.

4. Conditions of numerical simulation

4.1. Modeling the ship and port

This coal terminal was originally designed for 60,000 DWT (Deadweight) class coal carriers. However, recently, 90,000 DWT class ships have mainly been docking because of the trend of increasing ship size. Current mooring arrangement is obviously unbalanced in Fig. 6. In particular, the relatively short lines can be a risk of accidents because the mooring force can be concentrated (ATSB, 2008; Van der Molen et al., 2015). Numerical simulations were performed for 90,000 DWT coal carriers that were mainly berthed at T Port. The main dimensions of the modeled ship are shown in Table 2.

When ships are moored in port or offshore, horizontal motions, such as surge, sway, and yaw motions, become dominant. Thus, these three modes of motion are focused on in this study. In addition, the definition of the mooring line is determined by its location and role, as shown in Fig. 6.

The target vessel has usually used a 60 mm diameter PP ropes. The performance curve of ropes appears differently depending on the material of the rope. The load-elongation characteristics of each specific mooring rope of PP and HMPE are shown in Fig. 7. In addition, buckling type fenders are installed in this port to reduce the ship motions during cargo operation. The fenders were placed against the ship, with a height of 1600 mm and a length of 1100 mm. A total of seven fenders are located with an elastic limit for the reaction force of 1253 kN at 60% deflection, as shown in Fig. 7.

4.2. Rough wave condition

The records of offshore anchoring due to rough waves from 2015 to 2018 are summarized in Table 3. During the 4 years, there were 18 cases over 61 days. Offshore anchoring was considered necessary in these cases because the wave condition was forecasted to be Level 2 or 3. Therefore, it is possible to prevent dangerous situations.

Table 4 shows the records of dangerous cases with unexpected mooring risk from 2015 to 2018. This study defines “unexpected mooring risk” as the probabilistic risk associated with mooring accidents when forecasted in Level 1. During this period, 20 cases with unexpected mooring risk occurred over 60 days. These cases were expected to allow safe cargo operation. However, they were reported to have mooring difficulties due to unexpected rough seas in reality.

Table 2
Main dimension of 90,000 DWT coal carrier.

Classification	90,000 DWT coal carrier
Length overall (LOA)	235.00 m
Length between perpendiculars (LPP)	230.00 m
Breadth	43.00 m
Depth	18.40 m
Actual draft (half loaded)	10.76 m

Furthermore, there was an emergency evacuation due to large ship motions in Case P-7. In an emergency situation, the assistance of tug boats is immediately necessary. However, the tugboats are located an hour away from this port, so the only safety measure is to add mooring ropes in this port. However, since these measures are not sufficient, additional countermeasures are essential for safe port operation. The relation of wave heights between long-period waves and significant waves for the T Port is summarized in Fig. 8.

It is obvious that $H_{L1/3}$ exceeds 0.1–0.2 m, which makes large ship motions, even if $H_{1/3}$ is below 0.3–0.5 m inside the harbor in Fig. 8(B). In Fig. 8(A), wave heights exceed the safety criteria in many cases. However, it is obvious that many records of the wave heights are below the safety range, owing to the overestimated forecasting in this port. Therefore, it is possible to increase the efficiency of port operation by reducing such inappropriate mooring delays.

Among the total cases affected by the rough waves in Tables 3 and 4, the typical cases are selected. Fig. 9 shows the time history for the height of significant waves and long-period waves for the typical cases. The significant wave height is about 0.43–1.33 m, and the long-period wave height is about 0.23–0.97 m. The wave height of these cases exceeds the operational criteria of wave height. Therefore, it is shown that mooring difficulties could occur during these periods.

4.3. Mooring arrangement

In this study, numerical simulations of moored ship motions were conducted for the suggested mooring Methods (A)–(C) with the present method, as shown in Fig. 10.

The present method refers to the unbalanced condition of the current mooring arrangement with synthetic fiber ropes. Method (A) indicates the mooring method using the synthetic fiber rope with the revised mooring arrangement as the symmetrical one. In Method (B), although the mooring arrangement is the same as that in the present method, the HMPE is used instead of the synthetic

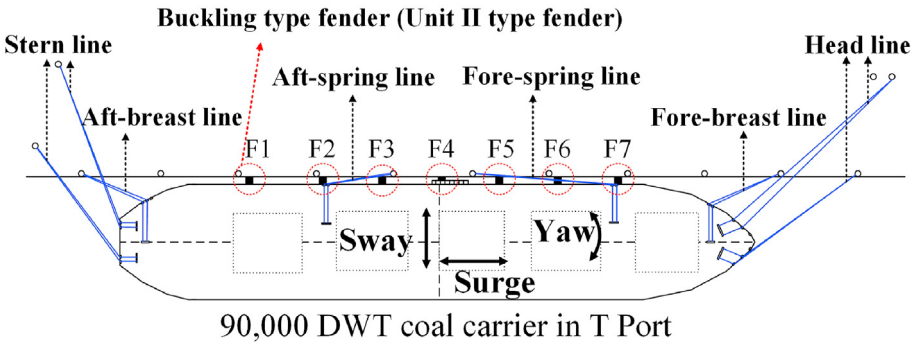

Fig. 6. Current mooring arrangements and description of the mooring facilities in T Port.

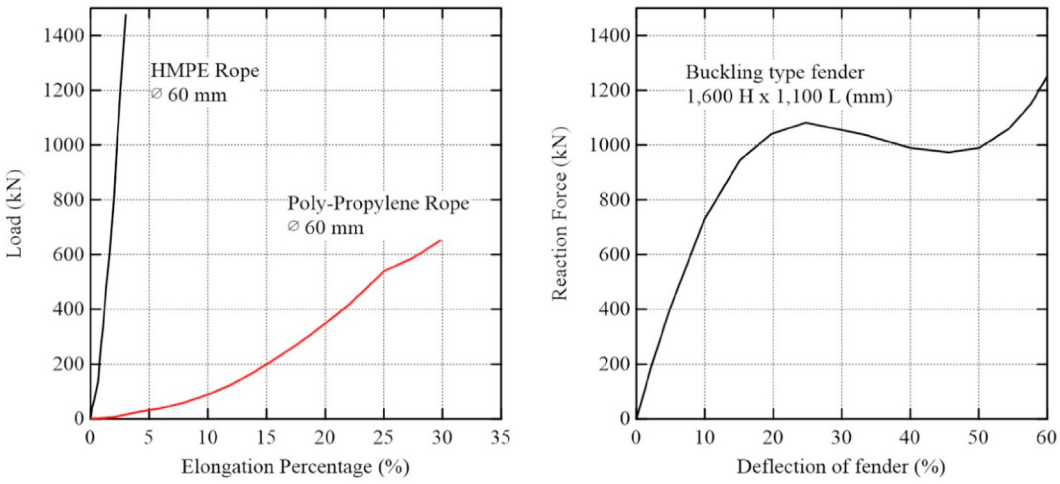

Fig. 7. Load-elongation characteristics of mooring ropes (HMPE and PP ropes) and reaction force-deflection of buckling type fenders.

Table 3
Record of offshore anchoring due to rough weather forecasting (2015–2018).

Case	Waiting period	Maximum $H_{1/3}$ (Inside harbor)	Maximum $H_{L1/3}$ (Inside harbor)	Weather condition
O-1	2015-11-26–2015-11-28	0.74 m	0.33 m	Low pressure
O-2	2016-01-15–2016-01-20	1.33 m	0.97 m	Low pressure
O-3	2016-05-02–2016-05-05	0.76 m	0.34 m	Low pressure
O-4	2016-08-06–2016-08-11	1.05 m	0.77 m	Typhoon
O-5	2016-08-29–2016-09-01	2.31 m	1.65 m	Typhoon
O-6	2017-03-13–2017-03-14	0.46 m	0.18 m	Low pressure
O-7	2017-04-17–2017-04-20	1.02 m	0.62 m	Low pressure
O-8	2017-09-19–2017-09-20	1.16 m	0.66 m	Typhoon
O-9	2017-10-07–2017-10-09	0.58 m	0.38 m	Low pressure
O-10	2017-12-12–2017-12-13	0.71 m	0.08 m	Low pressure
O-11	2018-01-22–2018-01-24	0.78 m	0.18 m	Low pressure
O-12	2018-03-02–2018-03-03	1.08 m	0.37 m	Low pressure
O-13	2018-03-09–2018-03-11	0.42 m	0.23 m	Low pressure
O-14	2018-03-21–2018-03-24	0.25 m	0.14 m	Low pressure
O-15	2018-04-12–2018-04-13	0.55 m	0.13 m	Low pressure
O-16	2018-05-02–2018-05-04	0.25 m	0.14 m	Low pressure
O-17	2018-05-17–2018-05-20	0.23 m	0.12 m	Low pressure
O-18	2018-10-25–2018-10-30	1.01 m	0.23 m	Low pressure

Table 4
Record of dangerous cases with unexpected mooring risk (2015–2018).

Case	Staying period in port	Maximum $H_{1/3}$ (Inside harbor)	Maximum $H_{L1/3}$ (Inside harbor)	Weather condition	Visual report (Ship motions)
P-1	2015-11-15–2015-11-17	0.63 m	0.22 m	Low pressure	Small
P-2	2015-12-11–2015-12-13	0.48 m	0.26 m	Low pressure	Small
P-3	2016-02-21–2016-02-23	0.97 m	0.25 m	Low pressure	Small
P-4	2016-04-13–2016-04-15	1.04 m	0.19 m	Low pressure	Small
P-5	2016-04-15–2016-04-17	1.04 m	0.37 m	Low pressure	Small
P-6	2016-04-27–2016-04-29	0.54 m	0.22 m	Low pressure	Small
P-7	2016-06-18–2016-06-21	0.71 m	0.34 m	Low pressure	Large
P-8	2016-07-31–2016-08-02	0.43 m	0.23 m	Typhoon	Small
P-9	2016-09-22–2016-09-24	0.51 m	0.25 m	Typhoon	Small
P-10	2016-12-13–2016-12-15	1.45 m	0.24 m	Low pressure	Small
P-11	2017-02-06–2017-02-08	0.49 m	0.23 m	Low pressure	Middle
P-12	2017-02-24–2017-02-26	1.17 m	0.22 m	Low pressure	Middle
P-13	2017-07-23–2017-07-25	0.50 m	0.31 m	Typhoon	Small
P-14	2017-07-25–2017-07-27	0.44 m	0.27 m	Typhoon	Small
P-15	2017-09-29–2017-10-01	1.11 m	0.16 m	Typhoon	Small
P-16	2017-10-29–2017-10-31	0.87 m	0.30 m	Low pressure	Small
P-17	2018-08-01–2018-08-03	0.25 m	0.08 m	Low pressure	Small
P-18	2018-08-16–2018-08-18	0.19 m	0.13 m	Low pressure	Small
P-19	2018-08-26–2018-08-28	0.45 m	0.16 m	Typhoon	Small
P-20	2018-12-05–2018-12-07	0.58 m	0.11 m	Low pressure	Small

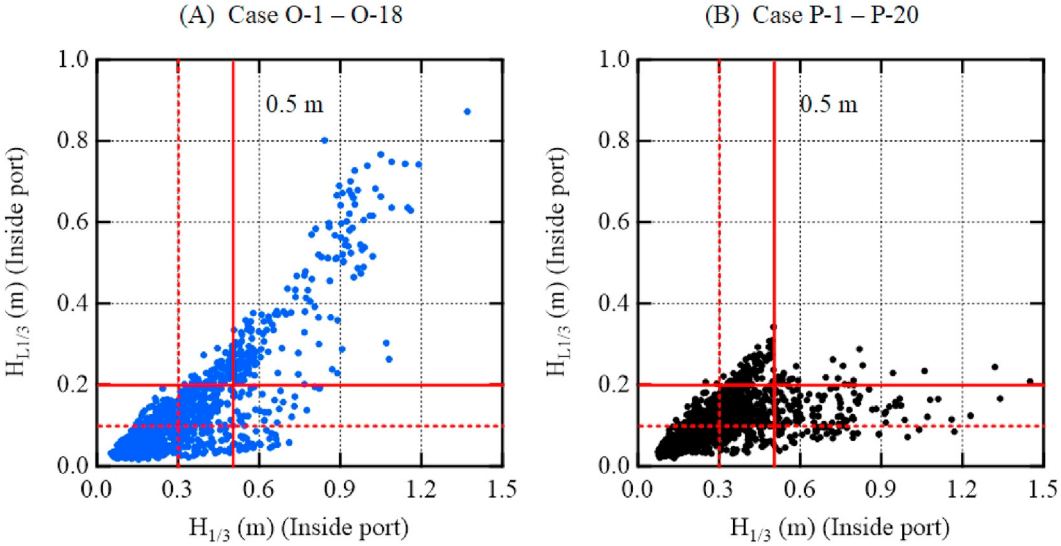

Fig. 8. Relation between the long-period and significant waves in 2015–2018.

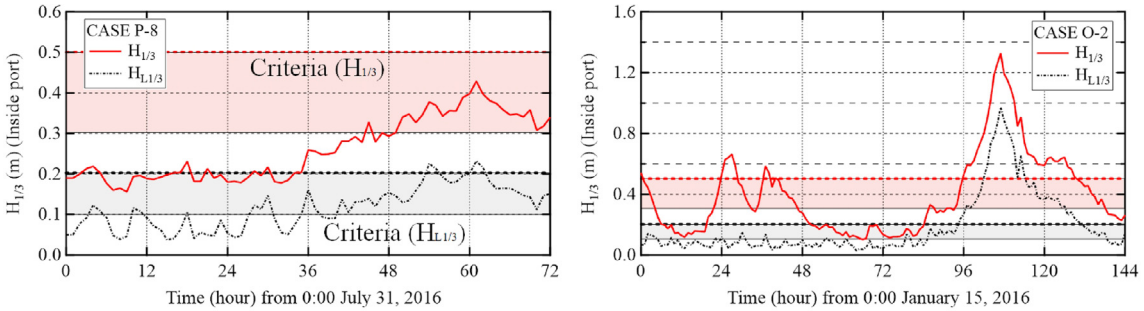

Fig. 9. Time history of the significant wave height in typical cases (Case P and Case O).

fiber rope. As the HMPE rope has very little elongation, the end-part of the HMPE rope is connected to the 11 m nylon tail rope to absorb the tension. Method (C) refers to the symmetrical mooring arrangement using the HMPE rope with a nylon tail rope. Comparing the present method with each suggested mooring Methods (A)–(C), the main purpose of the simulation is to verify the optimal mooring method in terms of safety and economic efficiency.

5. Results and discussion

5.1. Analyzed results of moored ship safety

In this study, the total cases affected by rough waves (20 cases with unexpected mooring risk, and 18 cases for offshore anchoring) were simulated and analyzed for verification of mooring safety. Here, the simulation results of typical cases are shown as examples. The heights of the significant wave and long-period waves for the typical examples (Case O and Case P) are shown in Fig. 9.

5.1.1. Case O

Case O is one of the cases of offshore anchoring due to rough sea forecasting. The ship arrived at the T Port on January 15, 2016. However, because rough waves were forecasted, the berthing schedules were delayed according to the berthing operation guidelines. In this study, the simulation was conducted for the first 72 h under the assumption that there is no offshore anchoring.

Variations of moored ship motions and fender deflections are analyzed in January 15–20, 2016, as shown in Fig. 11. The World Association for Waterborne Transport Infrastructure (PIANC) guidelines for criteria of moored ship motions for bulk carriers with a conveyer belt operation are 5 m for surge, 2.5 m for sway, and 3° for yaw (PIANC, 1995). These criteria for each parameter are represented by the red line in the figure.

In Fig. 11, the maximum amplitudes of surge, sway, and yaw motions exceed the criteria in the present method and Method (A), while the maximum amplitude is under the criteria in Methods (B) and (C). This indicates that the application of the HMPE rope is effective in reducing ship motions. However, the amplitude of motions did not significantly change according to the mooring arrangements. Meanwhile, the fender deflections do not exceed the safety criteria in all methods. Deflection of the fenders is not significantly different from mooring methods.

Variations in the safety parameters for mooring ropes, such as *PBT* and *TEMP* are analyzed from January 15–20, 2016, as shown in Fig. 12. The safety criteria for a rope tension are set at 50% of the break strength (OCIMF, 2018). In addition, the safety criteria for temperature are set at 60 °C based on the studies of TTI and Nobel Denton (1999) and McKenna et al. (2004). *PBT* shows that the value of the fore-breast line only approaches the safety limit in Method (B). *PBT* of the other line is within the safe range. The reason for the high tension of the fore-breast line in Method (B) is related to the

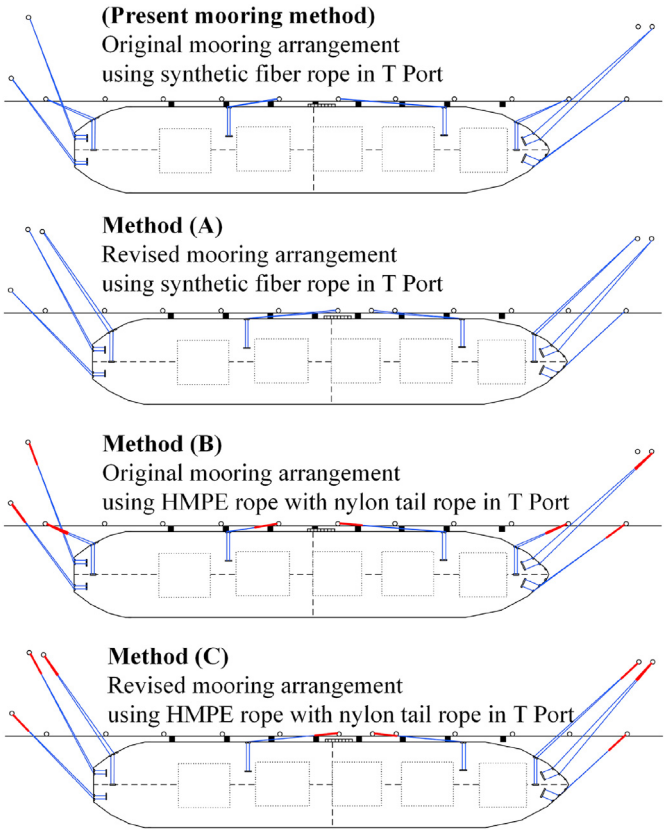

Fig. 10. Present mooring method and the suggested mooring methods.

mooring arrangement. The mooring arrangement in Method (B) shows very short fore-breast lines. In order to reduce the large ship motions, the kinetic energy of ship motions generated from rough waves must be absorbed by the fore-breast lines consisting of HMPE ropes in Method (B).

In addition, the variation in the maximum temperature of the rope is shown in Fig. 12. In the temperature analysis, the fore-spring line in Method (A) and aft-breast line in the present method are evaluated as dangerous because they exceed the safety range of 60 °C. Nevertheless, Method (C) is the only method evaluated as safe, as it meets all safety criteria. Comprehensively, Method (C) only shows the safe mooring in this example, Case O, resulting in the cancellation of offshore anchoring.

5.1.2. Case P

Case P is one of the cases with unexpected mooring risk. The ship arrived on July 31, 2016 and directly berthed at this port. The wave forecast services expected safe conditions. However, the wave conditions were rough enough to create dangerous mooring situations.

Variations in moored ship motions and fender deflections were analyzed from July 31 to August 2, 2016, as shown in Fig. 13. With the PIANC guidelines, the simulation shows that the present method and Method (A) using PP ropes exceeds the criteria. However, Methods (B) and (C) with HMPE rope show that the moored ship can stay within safety limits. Meanwhile, the fender deflections do not exceed the safety criteria in any of the methods. Variations of safety parameters for mooring ropes from July 31 to August 2, 2016, are analyzed in Fig. 14. It is clear that the tension of the fore-breast and aft-breast lines exceed the safety criteria in Method (B), and the tension of the aft-breast line exceeds the safety criteria in the present method. However, the values are less than the safety criteria in Method (C).

With the effects of friction and bending fatigue, the value of *TEMP* is higher when using synthetic fiber rope than when using HMPE rope. It is shown that the value of *TEMP* is related to rope materials. Although the values of *PBT* and *PBTF* of the fore-breast line exceed the criteria in Method (B), the value of *TEMP* is less than the criteria. In addition, the value of *TEMP* of the fore-breast line exceeds the criteria in the present method. The elongation of the ropes with ship motions is significantly reduced when using the HMPE ropes, which helps to maintain the low temperature of the ropes. For this reason, it is obvious that the adoption of HMPE ropes can be advantageous for safety from the viewpoint of temperature.

5.2. Evaluation from the viewpoint of safety

The decision of berthing is based on reliable wave forecasting in the case of the T Port. However, the wave forecast cannot be perfect and sometimes leads to incorrect decisions. These inappropriate mooring situations occur when the wave force is underestimated or not considered. Therefore, it is necessary to verify the optimal mooring method from a safety point of view by analyzing these mooring situations.

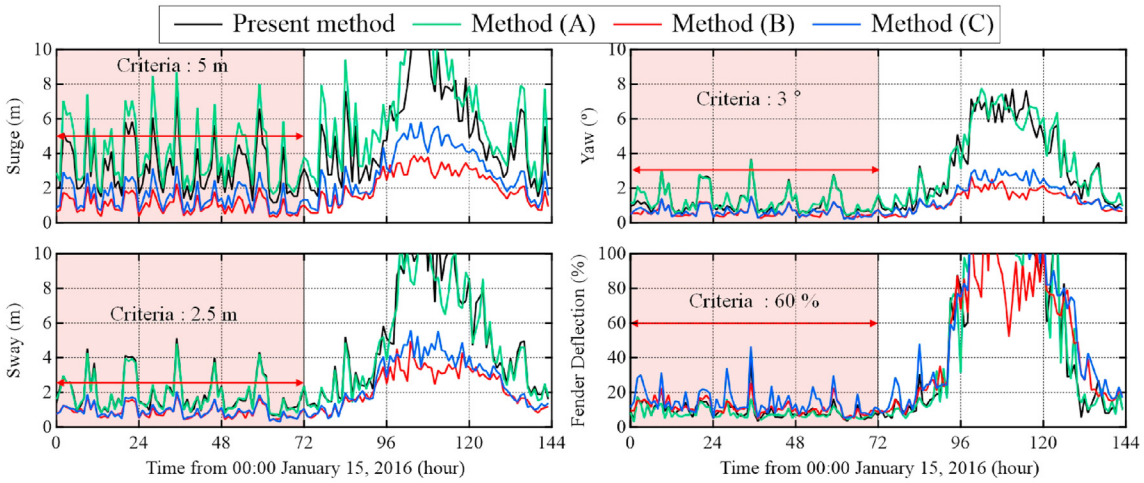

Fig. 11. Variations of moored ship motions (surge, sway, and yaw) and fender deflections for January 15–20, 2016 (CASE O).

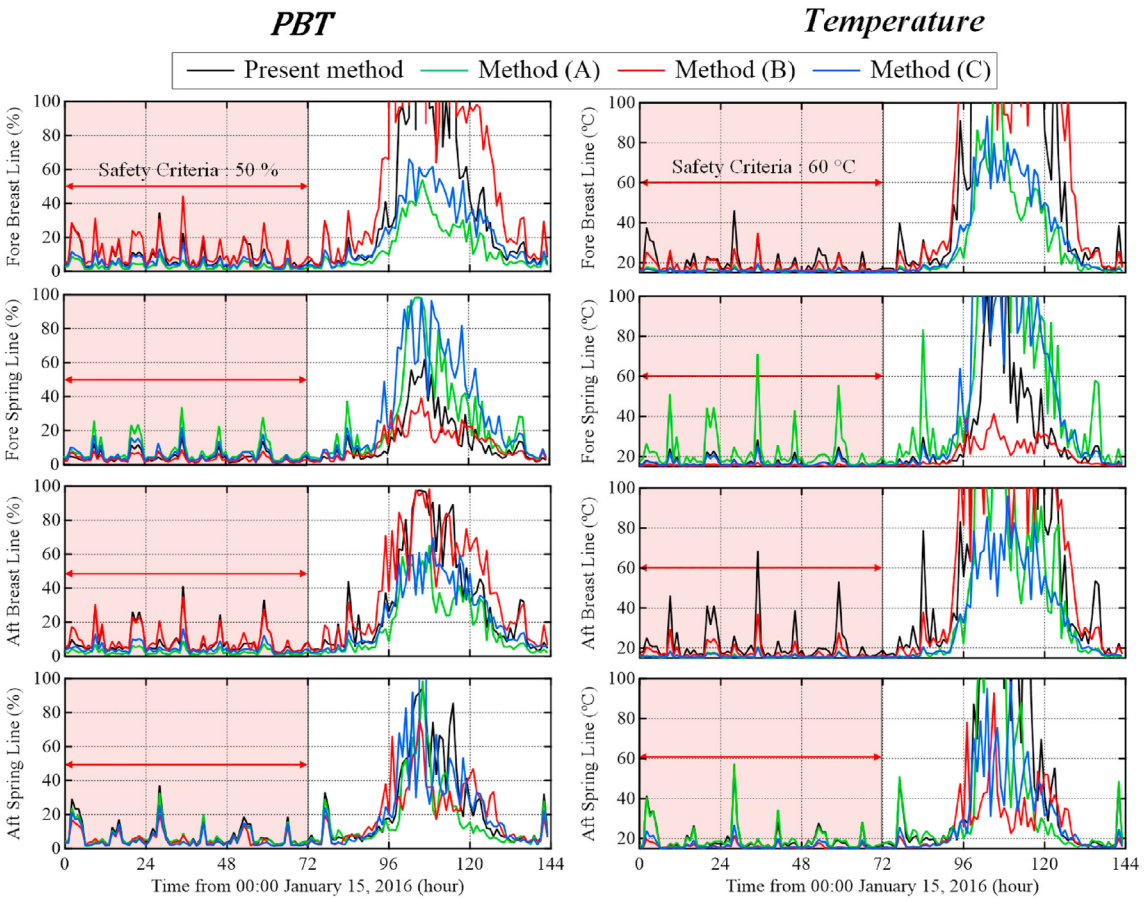

Fig. 12. Variations of the evaluation of mooring ropes for January 15–20, 2016 (CASE O).

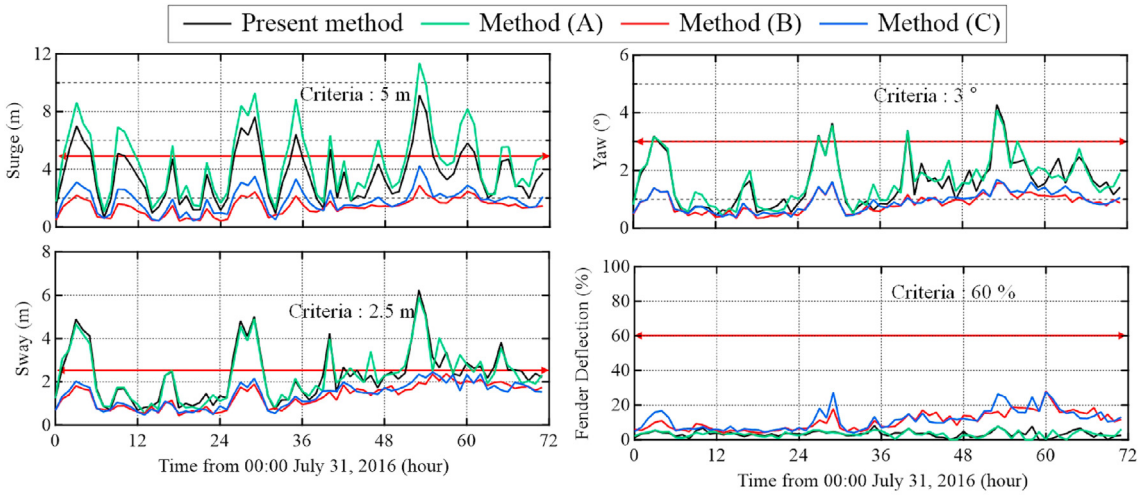

Fig. 13. Variations of moored ship motions (surge, sway, and yaw) and fender deflections from July 31 to August 2, 2016 (CASE P).

The simulation results are analyzed and compared with the present method and suggested mooring Methods (A)–(C). The relationships between long-period wave heights and maximum amplitude from the simulated results of 2736 h (=38 cases × 72 h) for 38 cases in 2015–2018 are shown in Fig. 15. In addition, the red lines in the figure indicate the safety criteria, which are 50% for tension and 60 °C for temperature. In Fig. 15, it is obvious that the least dangerous mooring situations that exceed safety criteria are in Method (C). However, Methods (A) and (B) are not significantly different from the present method.

In terms of safety, the maximum amplitude of each evaluation method is compared with the safety criteria. If the simulated value of each operation hour exceeds the safety criteria, the operation hours are defined as the dangerous hours with mooring risk. For

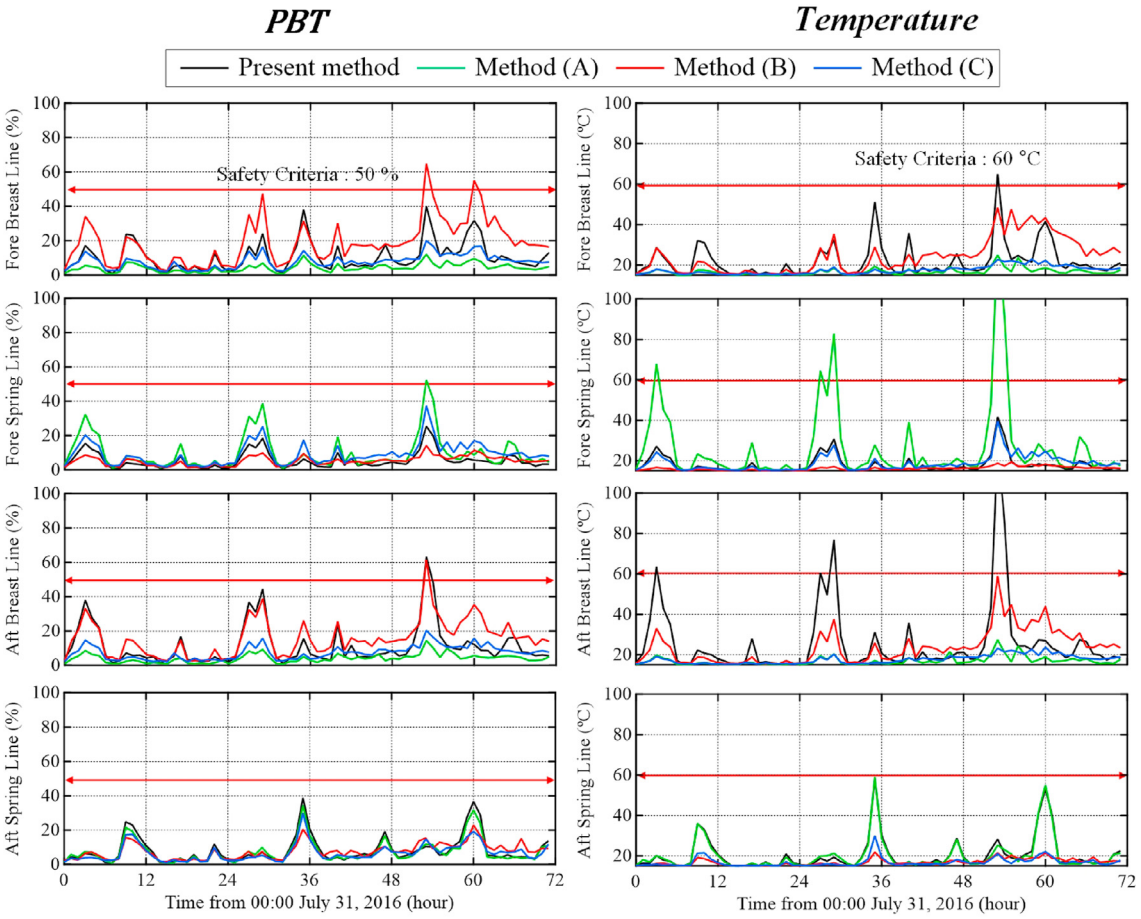

Fig. 14. Variations of evaluation of mooring rope from July 31 to August 2, 2016 (CASE P).

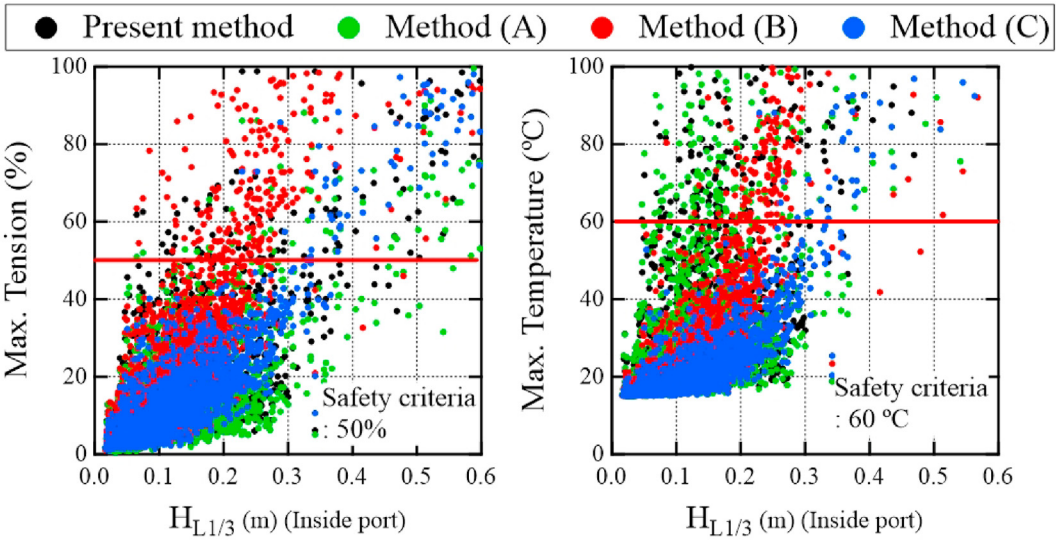

Fig. 15. Relations between the long-period wave heights and maximum amplitude of tension and temperature of mooring ropes in 2015–2018.

the 72 h of every case, it is analyzed whether the operation is dangerous or not. The portion of dangerous hours with mooring risk within total operation hours, *PDM*, can be obtained as follows:

$$PDM(\%) = \frac{H_d}{H_o}, \tag{14}$$

where H_o is the total operation hours in port, and H_d is the

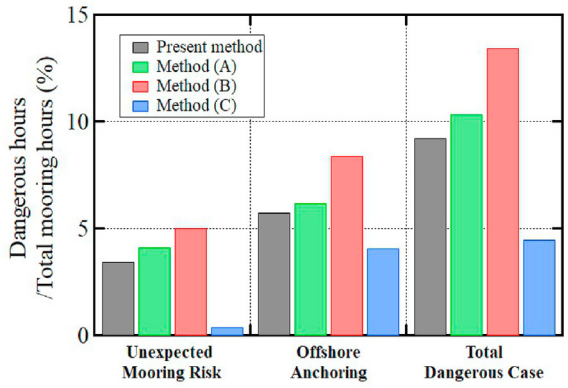

Fig. 16. Portion of dangerous hours from the total mooring period according to the suggested mooring Methods (A)–(C) in 2015–2018.

dangerous mooring hour with mooring risk, which exceeds the safety criteria. Comparing the value of *PDM* in each mooring method, it is possible to verify the low-risk mooring method. Using this concept, each mooring method can be compared objectively, and the optimal mooring methods in rough waves can be verified. The results of the mooring safety evaluation in all cases are shown in Fig. 16.

The results of the present method and Method (A) are similar. It is shown that these two methods are nearly equal in the total portion of high risk (10%). However, Method (B) is the most dangerous in this evaluation because the result shows the largest proportion of high risk (13%). In contrast, the operation hours using Method (C) are only exposed to dangerous situations for less than 5% of the total operation hours. In particular, the dangerous hours are only 11 h (0.4%) in the case with an unexpected mooring risk. The results show that Method (C) is most effective in terms of safety.

5.3. Evaluation from the viewpoint of cost-benefit performance

Based on the field survey, including literature review, the main priority of port operation can be categorized into two aspects. These are safety and economic efficiency. Safety is the standard for how safe the moored ship is to stay without any difficulties. Economic efficiency refers to how efficiently the moored ship can be operated without significant delay due to rough sea. However, there are no effective evaluation methods for the mooring facility that balance finance with safety. This point is very important to solve the mooring problem in the current situation. From these points of view, the berthing delay is validated by enhancing the mooring methods.

To verify the possibility of berthing, the evaluation of mooring safety is focused on checking whether the result exceeds the safety criteria during the first 72 h. If the simulation result exceeds these safety limits, the demurrage cost cannot be reduced because the berthing is impossible. If the simulation result is less than these limits, the ship could reduce the demurrage cost because berthing is possible.

In fact, the actual berthing delay due to rough waves is a total of 61 days over 4 years in the T Port. However, this simulated result is different for each mooring method, as shown in Table 5. In addition, there is a difference of 20 days between the simulation results and reality in the present method. These 20 days of berthing delay are caused by overestimated weather forecasting. If the forecasting accuracy is 100%, the present method can reduce the berthing delay by 20 days. Through the difference of these 20 days, it can be estimated that the error of the current weather forecasting system is approximately 33% (0.33 = 1–41/61).

Using the mooring Methods (A) and (B), the results show berthing delays of 43 and 52 days, respectively. This result indicates that the two methods for economic efficiency are not effective than the present method because they cannot reduce the berthing delay. Method (C) shows only 22 days of berthing delay, which is the only efficient from the economic aspect.

As mentioned, it is very important to discuss the reduced cost by enhancing the mooring systems, as shown here. Methods (A)–(C) require the cost of initial investment and an additional maintenance cost to introduce the new mooring system. However, it is shown that Methods (A) and (B) are not worth it to consider economic efficiency because both these methods increase the berthing delay. Therefore, the economic effect should be verified only for Method (C) by considering these investment and extra maintenance costs for additional facilities. Basically, maintenance costs for the present method are required for other methods, too. However, the additional cost of maintenance is only evaluated here by introducing the new mooring system. To evaluate the relationship between the accumulated cost of demurrage and the total investment cost of the new mooring system, the function of safety equipment and total payments, *FSTP*, is newly defined here.

$$FSTP = \sum_{i=1}^{N} D_i + \sum_{i=1}^{N} (I_i + M_i), \tag{15}$$

where D_i is the accumulated cost of demurrage (delay) per year, I_i is the investment cost of the initial construction and the renewal of the mooring system (every 20 years), and M_i is the additional maintenance cost due to the enhanced mooring system (every five years). N is the operation periods (years).

For the accumulated cost of demurrage, it is necessary to know the cost of demurrage per day. Based on the field survey in T Port, the daily cost of demurrage is set at $40,000. Thus, the total accumulated cost of demurrage D_i can be obtained for the present method and Method (C) as in Table 6. For example, the present method shows 61 days of delays for 4 years in reality. This means that the delay occurs on an average for 15.25 days every year. Therefore, multiplying this average by the daily cost of demurrage ($40,000), the annual loss D_i of the present method is $0.61 million.

Method (C) requires investment cost I_i of bitt installation ($0.5 million = 2 sets × $250,000), rope replacement ($0.44 million = 22 sets × $20,000), and installation of a shore winch ($2.4 million = 6 sets × $400,000). The additional maintenance cost M_i is set to $0.1 million per five years in Method (C). The parameter values of D_i, M_i, and I_i for the present method and Method (C) are summarized in Table 6.

Variations in *FSTP* are compared between the present method and Method (C) if the life cycle of the port is assumed to be 60 years.

Table 5
Total delay in the actual and simulated result for suggested mooring Methods (A)–(C) in 2015–2018.

Total delay	Present	Method (A)	Method (B)	Method (C)
Actual delay	61 days	–	–	–
Simulation result of delay (100% of forecasting accuracy)	41 days	43 days	52 days	22 days

Table 6
Parameter values for the function of safety equipment and total payments.

Parameter	Present method	Method (C)
D_i (Current weather forecasting)	$0.61 million/year	$0.42 million/year
D_i (100% accuracy weather forecasting)	$0.41 million/year	$0.22 million/year
M_i	–	$0.10 million/5 years
I_i	–	$3.34 million/20 years

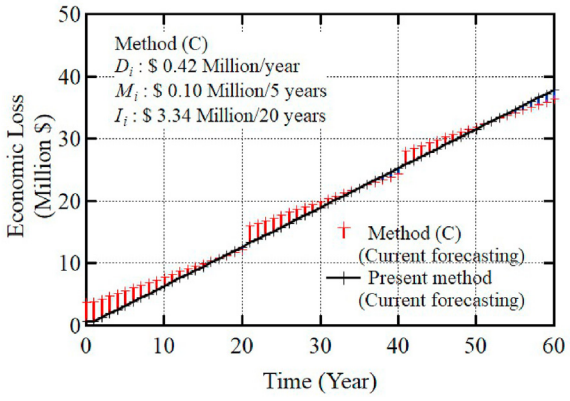

Fig. 17. Function of safety equipment and total payments with the current weather forecasting systems.

Fig. 17 shows the result of *FSTP* with the current forecasting system. The black line shows the accumulated loss of the present method. The present method has an annual economic loss of $0.61 million without any investment and additional maintenance cost, resulting in $36.6 million after 60 years. Although Method (C) required initial investment costs due to the enhanced mooring system, the total cumulative loss was $36.3 million. The investment cost is finally compensated for and leads to profits after 20 years.

In addition, if 100% of weather forecasting is possible with the development of a weather forecasting technology, the variations in *FSTP* can be described as shown in Fig. 18. Here, the *FSTP* of Method (C) with 100% forecasting accuracy can be compared with two cases of the present method (current and 100% forecasting accuracy). In Fig. 18(A), since both the present method and Method (C) are assumed to have 100% forecasting accuracy, each mooring method shows the total accumulated loss of $24.6 million and $24.3 million, respectively. However, if compared with the present method including the current forecasting error (20 days, 33%), Method (C) with advanced forecasting shows admirable economic efficiency, as shown in Fig. 18(B). The cumulative economic benefits gradually increase over time, resulting in a total accumulated benefit of $12.6 million after 60 years. It shows that the enhanced mooring method with the improvement in weather forecast accuracy can contribute to significantly reducing the economic loss of a moored ship.

According to the field survey, some port operators do not hesitate to invest in safety as a top priority, regardless of how much the cost is necessary. However, many domestic port operators cannot afford to invest in the reinforcement of port facilities. In this study, Method (C) is verified as the optimal mooring method in the T Port. This proposed method requires a large budget for initial investment. However, this initial investment can be recovered by reducing the demurrage cost of offshore anchoring. Moreover, this improvement in port facilities can increase the allowable wave height, increasing the efficiency of port operations. In addition, the extra benefit can be expected from the development of weather forecasting technology.

In this study, the suggested mooring method (C) is verified to be effective and sufficiently applicable not only for the improvement of port safety but also for financial advantage in the long term. However, because these results are for the target terminal only, the results could be different depending on the mooring situation at other ports. Therefore, it is necessary to conduct additional analyses with other port terminals in future studies.

6. Conclusions

In this study, new evaluation methods were proposed to reduce the risk of a moored ship. Friction and bending fatigue were newly included in the analysis of mooring ropes. This method seems more effective and accurate because it considers the rope-breaking mechanism. In addition, optimal mooring methods were verified in terms of safety and economic efficiency. This study is summarized as follows.

(1) Simulated results show that accumulated friction generates heat and damages the rope. Therefore, it was necessary to

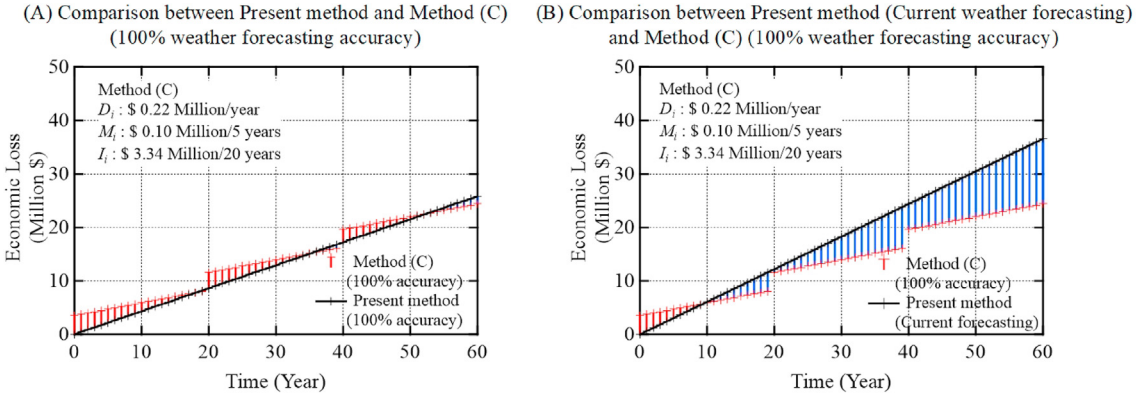

Fig. 18. Function of safety equipment and total payments with 100% accuracy of the weather forecasting systems.

analyze friction, bending fatigue, and temperature, in addition to a tension analysis.

(2) Moored ship motion was compared among mooring Methods (A)–(C). The optimal mooring method from the safety point of view is one that maintains the lowest dangerous mooring hours. As a result, since Method (C) had the lowest number of dangerous hours, it was considered optimal in terms of safety.

(3) The *FSTP* was newly introduced to confirm economic efficiency. It is defined as total costs including investment, maintenance, and demurrage. It enables one to estimate the amount of total costs. Methods (A) and (B) showed negative effects, which meant that their economic efficiency was not sufficient. Method (C) showed economic benefits among the three suggested mooring methods.

(4) As a result of checking with the proposed evaluation methods in terms of safety and economic efficiency, Method (C), a balanced mooring arrangement with a HMPE rope, was verified as the optimal mooring method. Moreover, economic efficiency can be expected to reach maximum benefit with the development of weather forecasting technology.

(5) This study is expected to help port terminals experiencing mooring problems in terms of economic efficiency and safety. It is necessary to verify these results through actual measurements in further research. A further analysis of mooring safety must also be conducted for different port regions, weather conditions, ship types, etc.

Declaration of competing interest

The authors declare that they have no known competing financial interests or personal relationships that could have appeared to influence the work reported in this paper.

Acknowledgement

The authors would like to express their appreciation to Capt. Tomiaki Oribe and Capt. Takayuki Nakajima, of the Tomato Coal Center Co. Inc., Japan, for offering us access to many important databases and documents on the ship mooring of 90,000 DWT class coal carriers. We also wish to show our appreciation to the Hokkaido Electric Power Co., Inc., Japan, for providing measured wave data inside the port. In addition, we express our appreciation to the Ministry of Land, Infrastructure, Transport and Tourism, Japan, for offering the measured wave data offshore from the port. This study could not have been conducted without their support. We express our gratitude to Mr. Koji Utsumi, Tesac Cooperation, Japan, Mr. Tetsuya Yamamoto, Naroc Rope Tech., Japan, and Mr. Stephen Dietz, Samson Rope Technologies, USA, for their guidance on rope strength and friction at sea. This study was financially supported by Scientific Research (B) (Project No. 20H02398, 2020–2024, represented by Kenji Sasa) under a Grant-in-Aid for Scientific Research, Japan Society for the Promotion of Science.

References

ATSB (Australian Transport Safety Bureau), 2008. Independent Investigation into the Breakaway and Grounding of the Hong Kong Registered Bulk Carrier Creciente at Port Hedland, Western Australia on 12 September 2006. Canberra. https://www.atsb.gov.au/publications/investigation_reports/2006/mair/mair232/.

Black, K., Banfield, S.J., Flory, J.F., Ridge, I.M.L., 2012. Low-friction, low-abrasion fairlead liners. In: Proc. OCEANS 2012 IEEE/MTS, pp. 1–11. https://doi.org/10.1109/OCEANS.2012.6405022. USA.

Bossolini, E., Nielsen, O.W., Oland, E., Sørensen, M.P., Veje, C., 2016. Thermal properties of Fiber ropes. In: Paper Presented at European Study Group with Industry, Denmark. https://orbit.dtu.dk/en/publications/thermal-properties-of-fiber-ropes.

Cummins, W.E., 1962. The Impulse Response Function and Ship Motions. David Taylor Model Basin, USA. Technical Report No. DTMB-1661.

Foster, G.P., 2002. Advantages of fiber rope over wire rope. J. Ind. Textil. 32 (1), 67–75. https://doi.org/10.1106/152808302031656.

González-Marco, D., Sierra, J.P., Fernández de Ybarra, O., Sánchez-Arcilla, A., 2008. Implications of long waves in harbor management: the Gijón port case study. Ocean Coast Manag. 51, 180–201. https://doi.org/10.1016/j.ocecoaman.2007.04.001.

Hashimoto, N., Kawaguchi, K., 2003. Statistical forecasting of long period waves based on weather data for the purpose of judgment of executing cargo loading. In: Proc. 13th Int. Soc. Offshore Polar Eng. Conf. Honolulu, USA, pp. 697–704. https://www.onepetro.org/conference-paper/ISOPE-I-03-302.

Hearle, J.W.S., Parsey, M.R., Overington, M.S., Banfield, S.J., 1993. Modelling the long-term fatigue performance of fibre ropes. In: Proc. 3th Int. Soc. Offshore Polar Eng. Conf. Singapore, pp. 377–383. https://www.onepetro.org/conference-paper/ISOPE-I-93-152.

Hobbs, R.E., Burgoyne, C.J., 1991. Bending fatigue in high-strength fibre ropes. Int. J. Fatig. 13 (2), 174–180. https://doi.org/10.1016/0142-1123(91)90011-m.

Ikeda, H., Yasuda, D., Yoneyama, H., Otake, Y., Hiraishi, T., 2011. Development of mooring system to reduce long-period motions of a large ship. In: Proc. 21th Int. Soc. Offshore Polar Eng. Conf. Hawaii, USA, pp. 1214–1221. https://www.onepetro.org/conference-paper/ISOPE-I-11-317.

John, F., 1950. On the motion of floating bodies II. Commun. Pure Appl. Math. 3 (1), 45–101. https://doi.org/10.1002/cpa.3160030106.

Karnoski, S.R., Liu, F.C., 1988. Tension and bending fatigue test results of synthetic ropes. In: Proc. Annual Offshore Tech. Conf. Houston, USA, pp. 343–350. https://doi.org/10.4043/5720-ms.

Kwak, M., Moon, Y., Pyun, C., 2012. Computer simulation of moored ship motion induced by harbor resonance in Pohang new harbor. In: Proc. 33rd Conf. Coast. Eng. Spain. https://doi.org/10.9753/icce.v33.waves.68.

Kubo, M., Barthel, V., 1992. Some considerations how to reduce the motions of ships moored at an open berth. J. Japan Inst. Nav. 87, 47–58. https://doi.org/10.9749/jin.87.47.

Kubo, M., Sakakibara, S., 1999. A study on time domain analysis of moored ship motion considering harbor oscillations. In: Proc. 9th Int. Soc. Offshore Polar Eng. Conf. France, pp. 574–581. https://www.onepetro.org/conference-paper/ISOPE-I-99-309.

López, M., Iglesias, G., 2014. Long wave effects on a vessel at berth. J. Appl. Ocean Res. 47, 63–72. https://doi.org/10.1016/j.apor.2014.03.008.

McKenna, H.A., Hearle, J.W.S., O'Hear, N., 2004. Handbook of Fibre Rope Technology. Woodhead Publishing, Cambridge.

MLIT (Ministry of Land, Infrastructure, Transport and Tourism), 2009. Technical Standards and Commentaries for Port and Harbour Facilities in Japan. Translated and edited by The Overseas Coastal Area Development Institute of Japan, Tokyo. http://ocdi.or.jp/en/technical-st-en.

Nabijou, S., Hobbs, R.E., 1995. Frictional performance of wire and fibre ropes bent over sheaves. J. Strain Anal. Eng. 30 (1), 45–57. https://doi.org/10.1243/03093247V301045.

Ning, F., Li, X., Hear, N.O., Zhou, R., Shi, C., Ning, X., 2019. Thermal failure mechanism of fiber ropes when bent over sheaves. Textil. Res. J. 89 (7), 1215–1223. https://doi.org/10.1177/0040517518767147.

OCIMF (Oil Companies International Marine Forum), 2018. Mooring Equipment Guidelines, fourth ed. Oil Companies International Marine Forum, London.

Overington, M.S., Leech, C.M., 1997. Modelling heat buildup in large polyester ropes. Int. J. Offshore Polar Eng. 7, 63–69, 01. https://www.onepetro.org/journal-paper/ISOPE-97-07-1-063.

PIANC (World Association for Waterborne Transport Infrastructure), 1995. Criteria for Movements of Moored Ships in Harbor: A Practical Guide. Brussels: PIANC General Secretariat.

Ridge, I.M.L., Wang, P., Grabandt, O., O'Hear, N., 2015. Appraisal of ropes for LNG moorings. In: Proc. OIPEEC Conf. 5th Int. Stuttgart Rope Days, Stuttgart, Germany. https://oipeec.org/products/appraisal-of-ropes-for-lng-moorings.

Sakakibara, S., Kubo, M., 2009. Initial attack of large-scaled Tsunami on ship motions and mooring loads. J. Ocean Eng. 36 (2), 145–157. https://doi.org/10.1016/j.oceaneng.2008.09.010.

Sasa, K., Kubo, M., Shiraishi, S., Nagai, T., 2001. Basic research on frequency properties of long period waves at harbour facing to the Pacific Ocean. In: Proc. 11th Int. Soc. Offshore Polar Eng. Conf. Stavanger, Norway, pp. 593–600. https://www.onepetro.org/conference-paper/ISOPE-I-01-322.

Sasa, K., 2017. Optimal routing of short-distance ferry from the evaluation of mooring criteria. In: Proc. Int. Conf. Offshore Mech. Arct. Eng. OMAE, vol. 6, pp. 1–8. https://doi.org/10.1115/OMAE201761077, 2.

Sasa, K., Mitsui, M., Aoki, S., Tamura, M., 2018. Current analysis of ship mooring and emergency safe system. J. Japan Soc. Civ. Eng. Ser. B2 (Coast. Eng.) 74 (2), 1399–1404. https://doi.org/10.2208/kaigan.74.I_1399 ([in Japanese]).

Sasa, K., Aoki, S., Fujita, T., Chen, C., 2019. New evaluation for mooring problem from cost-benefit effect. J. Japan Soc. Civ. Eng. Ser. B2 (Coast. Eng.) 75 (2), 1243–1248. https://doi.org/10.2208/kaigan.75.I_1243 ([in Japanese]).

Shiraishi, S., Kubo, M., Sakakibara, S., Sasa, K., 1999. Study on numerical simulation method to reproduce long-period ship motions. In: Proc. 9th Int. Soc. Offshore Polar Eng. Conf. France, pp. 536–543. https://www.onepetro.org/conference-paper/ISOPE-I-99-304.

Shiraishi, S., 2009. Numerical simulation of ship motions moored to quay walls in long-period waves and proposal of allowable wave heights for cargo handling

in a port. In: Proc. 19th Int. Soc. Offshore Polar Eng. Conf. Japan, pp. 1109–1116. https://www.onepetro.org/conference-paper/ISOPE-I-09-232.

Sloan, F., Nye, R., Liggett, T., 2003. Improving bend-over-sheave fatigue in fiber ropes. In: Proc. OCEANS 2003 IEEE/MTS, USA, pp. 1054–1057. https://doi.org/10.1109/oceans.2003.178486.

Tti, Noble Denton, 1999. Deepwater Fibre Moorings: an Engineers' Design Guide. Ledbury.

Van der Molen, W., Monárdez, P., van Dongeren, A.P., 2006. Numerical simulation of long-period waves and ship motions in Tomakomai port, Japan. Coast Eng. J. 48 (1), 59–79. https://doi.org/10.1142/S0578563406001301.

Van der Molen, W., Scott, D., Taylor, D., Elliott, T., 2015. Improvement of mooring configurations in Geraldton harbour. J. Mar. Sci. Eng. 4 (3) https://doi.org/10.3390/jmse4010003.

Van Essen, S., Van der Hout, A., Huijsmans, R., Waals, O., 2013. Evaluation of directional analysis methods for low-frequency waves to predict LNGC motion response in nearshore areas. In: Proc. Int. Conf. Offshore Mech. Arct. Eng. OMAE, vol. 2013. https://doi.org/10.1115/OMAE2013-10235.

Villa-Caro, R., Carral, J.C., Fraguela, J.Á., López, M., Carral, L., 2018. A review of ship mooring systems. Brodogradnja 69 (1), 123–149. https://doi.org/10.21278/brod69108.

Yamamoto, K., Kubo, M., Asaki, K., Kanuma, Y., 2004. An experimental research on internal stress of ropes under repeated load. J. Japan Inst. Nav. 112, 353–359. https://doi.org/10.9749/jin.112.353 ([in Japanese]).

Yamamoto, K., Kubo, M., Asaki, K., 2006. Comparison between numerical calculation and experimental results of temperature rise on rope under repeated load. J. Japan Inst. Nav. 116, 269–275. https://doi.org/10.9749/jin.116.269 ([in Japanese]).

Yamamoto, K., 2007. Basic Research on Preventing Breakage of Mooring Ropes. PhD Diss. Kobe University ([in Japanese]).

Yoneyama, H., Minemura, K., Moriya, T., 2017. A study on calculation methods of allowable wave heights of a moored ship in remote island ports. J. Japan Soc. Civ. Eng. 73 (2), 803–808. https://doi.org/10.2208/jscejoe.73.I_803 ([in Japanese]).